JCB Article

Human centromere chromatin protein hMis12, essential for equal segregation, is independent of CENP-A loading pathway

Gohta Goshima,[1] Tomomi Kiyomitsu,[1] Kinya Yoda,[2] and Mitsuhiro Yanagida[1]

[1]COE Research Project, Department of Gene Mechanisms, Graduate School of Biostudies, Kyoto University, Kyoto 606-8502, Japan
[2]Bioscience Center, Nagoya University, Nagoya 464-8601, Japan

Kinetochores are the chromosomal sites for spindle interaction and play a vital role for chromosome segregation. The composition of kinetochore proteins and their cellular roles are, however, poorly understood in higher eukaryotes. We identified a novel kinetochore protein family conserved from yeast to human that is essential for equal chromosome segregation. The human homologue hMis12 of yeast spMis12/scMtw1 retains conserved sequence features and locates at the kinetochore region indistinguishable from CENP-A, a centromeric histone variant. RNA interference (RNAi) analysis of HeLa cells shows that the reduced hMis12 results in misaligned metaphase chromosomes, lagging anaphase chromosomes, and interphase micronuclei without mitotic delay, while CENP-A is located at kinetochores. Further, the metaphase spindle length is abnormally extended. Spindle checkpoint protein hMad2 temporally localizes at kinetochores at early mitotic stages after RNAi. The RNAi deficiency of CENP-A leads to a similar mitotic phenotype, but the kinetochore signals of other kinetochore proteins, hMis6 and CENP-C, are greatly diminished. RNAi for hMis6, like that of a kinetochore kinesin CENP-E, induces mitotic arrest. Kinetochore localization of hMis12 is unaffected by CENP-A RNAi, demonstrating an independent pathway of CENP-A in human kinetochores.

Introduction

Centromeres are enigmatic chromosome structures essential for correct segregation of sister chromatids. In higher eukaryotes, centromere DNAs are large, in the range of megabases, often containing repetitious DNA sequences in condensed heterochromatin (Choo, 2001; Schueler et al., 2001). Even in insects, e.g., *Drosophila*, the functional size of a centromere is ~500 kb (Sun et al., 1997). In the budding yeast *Saccharomyces cerevisiae*, however, the functional size of the centromere is very small; construction of a series of artificial mini-chromosomes showed that functional centromeres could be in the range of ~200 bp, 2,000-fold smaller than that of *Drosophila* (Fitzgerald-Hayes et al., 1982). Even among fungi, the difference in functional centromere size is considerable. In the fission yeast *Schizosaccharomyces pombe*, the functional size of centromeres is within the range of 35–110 kb (Takahashi et al., 1992). This huge difference in centromere size between different organisms appears at first glance very difficult to fit to a uniform structural hypothesis for all eukaryotes.

We considered fission yeast as a model organism for understanding the centromeres of higher eukaryotes. The centromeres in *S. pombe* consisted of basically two types of domains (Takahashi et al., 1992). One is highly repetitive sequences located in the outer domains of the centromeres as well as at the mating type locus, whereas the others were either unique or specific to the inner central domains of centromeres. Micrococcal nuclease digestion assays revealed the existence of two classes of centromeric chromatin (Polizzi and Clarke, 1991; Takahashi et al., 1992). The central domains contain the specialized chromatin, which presented as a smeared nucleosome ladder after micrococcal nuclease digestion. The outer repetitive regions gave digestion patterns of regular ladders.

The presence of these two classes with distinct DNA sequence organization and chromatin structure in the fission yeast centromeres was substantiated with specific centromere protein distribution. Chromatin immunoprecipitation experiments showed that Mis6, an essential kinetochore-localized protein, was specifically present in the central

Address correspondence to Mitsuhiro Yanagida, Department of Gene Mechanisms, Graduate School of Biostudies, Kyoto University, Kita-shirakawa-Oiwakecho, Sakyo-ku, Kyoto 606-8502, Japan. Tel.: 81-75-753-4205. Fax: 81-75-753-4208. E-mail: yanagida@kozo.biophys.kyoto-u.ac.jp

G. Goshima's present address is Department of Cellular and Molecular Pharmacology, University of California, San Francisco, CA.

*Abbreviations used in this paper: RNAi, RNA interference; siRNA, small interfering RNA.

Key words: kinetochore; HeLa; RNAi; Mis12; CENP-A

The Journal of Cell Biology, Volume 160, Number 1, January 6, 2003 25–39
http://www.jcb.org/cgi/doi/10.1083/jcb.200210005

The Journal of Cell Biology

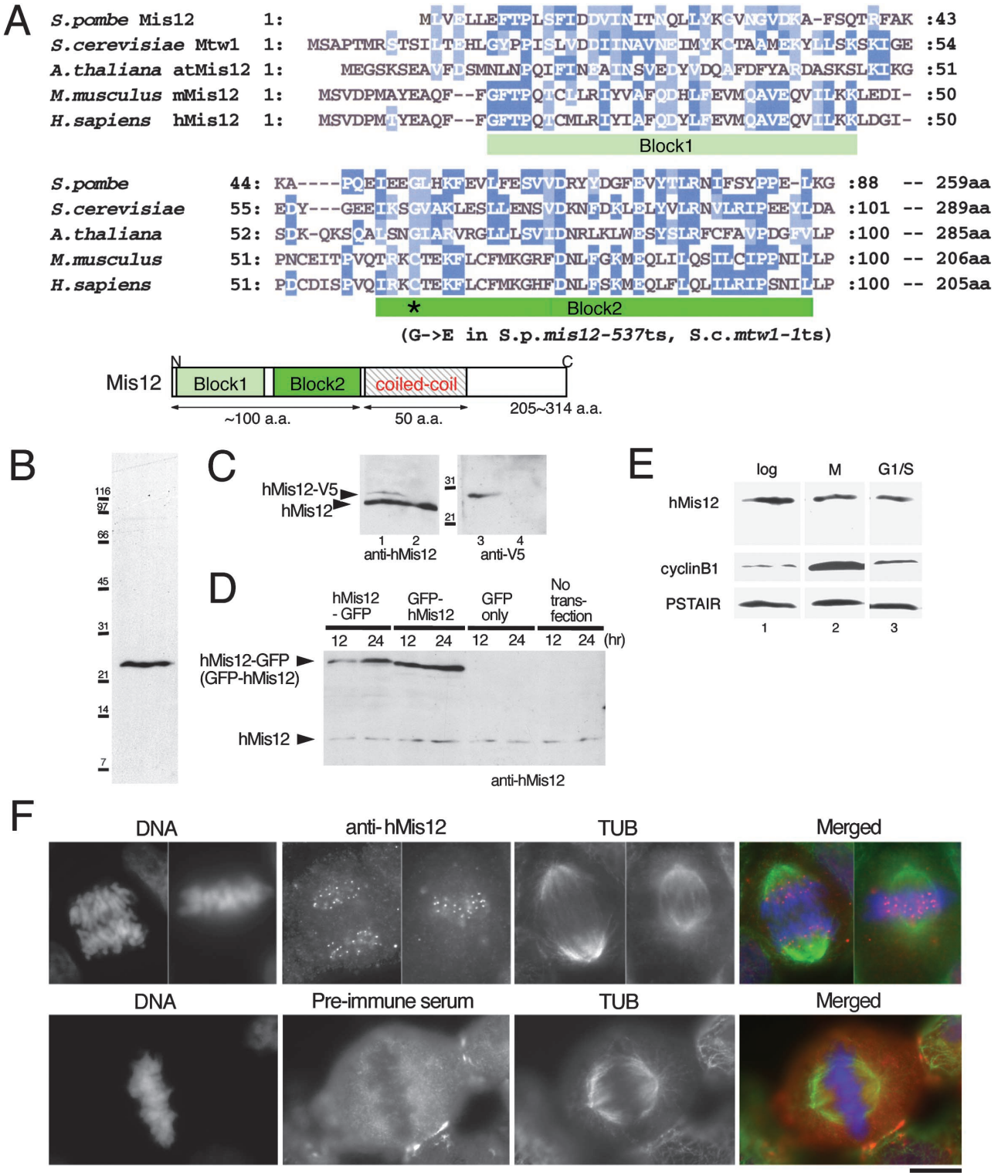

Figure 1. **Identification of hMis12.** (A, top) Alignment of the NH_2 terminus of Mis12-like proteins from *S. pombe* (Mis12), *S. cerevisiae* (Mtw1p), *A. thaliana* (atMis12; MOK9.12), *M. musculus* (mMis12; AK010995), *and H. sapiens* (hMis12; MGC2488). Identical amino acids are boxed and similar ones are hatched. The mutation site of *S. pombe mis12-537* ts and *S. cerevisiae mtw1-1* ts mutants is indicated (asterisk). (A, bottom) Schematic representation of the Mis12 family protein. The predicted coiled coil exists in the middle, while the two conserved regions (Block 1 and 2) are located in the NH_2-terminal 100 aa. (B) Identification of hMis12 protein in HeLa cell extract by immunoblotting using affinity-purified anti-hMis12 antibody. (C) The COOH terminus of the hMis12 gene was tagged with V5His6, and plasmid carrying hMis12–V5His6 under the CMV promoter was transfected into HeLa cells (lanes 1 and 3). Vector plasmid pcDNA3.1-V5His6 was transfected as control (lanes 2 and 4). Extracts were prepared 24 h after transfection, and immunoblotting was performed using anti-hMis12 (lanes 1 and 2) or anti-V5 (lanes 3 and 4) antibodies. 28-kD bands were detected in lanes 1 and 3. (D) GFP was tagged to the NH_2 terminus (GFP–hMis12) or COOH terminus (hMis12–GFP) of the hMis12 gene. The plasmid carrying GFP-tagged hMis12 under the CMV promoter was transfected into HeLa cells. Vector plasmid pEGFP-C1 was transfected as control. Extracts were prepared 12 and 24 h after transfection and immunoblotting

centromere region (Saitoh et al., 1997; Partridge et al., 2000). Mis12 and spCENP-A are also located in the same central region (Goshima et al., 1999; Takahashi et al., 2000). The loss of Mis6, Mis12, or spCENP-A induced random segregation of sister chromatids, consistent with the fact that the central centromere DNA region bound to these proteins was also essential for equal chromosome segregation. The outer centromeric regions were shown to be bound to Swi6, a heterochromatic protein resembling heterochromatin protein 1 (Partridge et al., 2000). A role of Swi6 is the incorporation of the cohesin complex essential for sister chromatid cohesion (Bernard et al., 2001; Nonaka et al., 2002). The loss of Swi6 function leads to a minor defect in chromosome segregation (Ekwall et al., 1995).

Fission yeast spMis6 was shown to be required for recruiting spCENP-A, a histone H3–like protein exclusively present in centromeres (Takahashi et al., 2000). CENP-A–containing nucleosomes may be responsible for the formation of specialized chromatin in the inner centromeres. Mis6 homologues are present in organisms from fungi to human. However, budding yeast Ctf3p and chicken CENP-I, Mis6 homologues, do not seem to be essential for CENP-A loading to the centromere (Measday et al., 2002; Nishihashi et al., 2002). Instead, Cse4p (CENP-A homologue) is needed for Ctf3p to be loaded onto the centromere in budding yeast. The loading relationship between mammalian Mis6 and CENP-A has not been reported so far.

The fission yeast mutation *mis12-537* displays a mis-segregation phenotype similar to *mis6-302* and leads to the lack of specialized centromere chromatin. But spMis12 seems to have functional independence of spMis6 (Goshima et al., 1999; Takahashi et al., 2000). No genetic interaction was found between these two genes, and localization was mutually independent: spMis12 was located at the centromere in *mis6* mutant cells, whereas both spCENP-A and spMis6 were located at the centromeres of *mis12* mutant cells. Immunoprecipitation using antibodies against spMis6 and spMis12 revealed no evidence for their physical interaction. Fission yeast spMis6 and spMis12 may thus function to form the specialized centromere chromatin through different pathways.

A BLAST search has revealed that Mis6, CENP-A, and many other kinetochore proteins are evolutionarily conserved from yeast to human. This leads to a prediction that kinetochore components might be largely common among eukaryotes in spite of their centromere DNA sequence variety. On the other hand, however, it is also true that many other kinetochore proteins discovered in fungi have obvious homologues only in fungi (Kitagawa and Hieter, 2001; Cheeseman et al., 2002). Mis12 was thought to be the latter case. Budding yeast has Mtw1, a homologue of spMis12, which is also localized at the kinetochore and whose loss leads to unequal segregation of chromosomes (Goshima and Yanagida, 2000), but no homologues could be found in higher eukaryotes. We therefore attempted to identify spMis12/Mtw1 homologues in higher eukaryotes. Here we show by advanced database search that Mis12 is conserved not only in fungi but also in plants and humans.

The human hMis12 first described in this report behaves as a kinetochore protein during mitosis and localizes in the kinetochore region in a pattern indistinguishable from that of CENP-A, hMis6, and CENP-C. Furthermore, the extensive use of the RNA interference (RNAi)* method (Fire et al., 1998; Elbashir et al., 2001) showed that the loss of hMis12 in HeLa cells induces the misalignment of chromosomes in metaphase, followed by the formation of lagging chromosomes in anaphase and micronuclei in interphase without apparent mitotic delay. The phenotypes predict the occurrence of chromosome missegregation.

Results

Identification of plant and human homologues of Mis12/Mtw1

Fission yeast spMis12 and budding yeast Mtw1 contain the conserved 100-aa NH_2 terminus, which consists of two highly conserved regions, block 1 and 2 (Fig. 1 A), immediately followed by the 50-aa presumed coiled coil. By BLAST search, however, homologous sequences with the meaningful E-value were not found in the genome of higher eukaryotes. We therefore employed the Block Maker (Henikoff et al., 1998; http://www.blocks.fhcrc.org/blocks/blockmkr/make_blocks.html) and MAST (Multiple Alignment and Search Tool; Bailey and Gribskov, 1998) for searching for similar genes under the conditions of two block sequences and one coiled-coil region. Three fungal homologues (*Candida albicans*, *Aspergillus nidulans*, and *Magnaporthe grisea)* and one *Arabidopsis thaliana* homologue (atMis12, MOK9.12; E-value = 0.058) have been obtained. *Arabidopsis* atMis12 also contained the 50-aa coiled coil after block 2. A similar gene was found in the bean *Glycine max* (sp43a06.y1). Using these five fungal and two plant Mis12 homologues for the Block Maker and MAST searching, we were able to obtain putative homologues of human (MGC2488; E-value = 1) and mouse (AK010995; E-value = 8.9), as shown in Fig. 1 A. Although the above E-values are much higher than those between Mis12 and Mtw1 (9e-08), all of them were in the range of 25–35 kD, containing two similar blocks and the 50-aa coiled coil. Databases of rat, bovine, and frog displayed proteins highly similar to hMis12. In fly, however, no putative homologue was found. *Caenorhabditis elegans* contained a potential homologue (Y47G6A.24; E-value = 8.1; RNAi of this gene leads to embryonic lethality; Maeda

was performed using anti-hMis12 antibody. 53-kD bands were additionally detected when GFP-tagged hMis12 was expressed. (E) No apparent change of hMis12 level in the cell cycle. HeLa cells were arrested at G1/S phase by double thymidine block (lane 3) or at M phase by nocodazole treatment (lane 2). Immunoblotting was performed using anti-hMis12, anti-cyclinB1, and anti-PSTAIR antibodies. CyclinB1 levels apparently increased in nocodazole-blocked M phase extracts. Extract from logarithmically growing cells was used as control (lane 1). (F) Kinetochore-like localization of hMis12. (F, top) Paraformaldehyde-fixed HeLa cells were stained by anti-hMis12 antibody (red) and anti-tubulin (green). hMis12 was localized on the M-phase condensed chromosomes showing many punctate signals. (F, bottom) No staining was observed on chromosomes when preimmune serum was used. DNA was stained by Hoechst 33342 (blue). Bar, 10 μm.

et al., 2001) but the similarity was low compared with other Mis12 homologues.

Identification of hMis12 protein

To detect hMis12 in cell extracts, rabbit polyclonal antibodies were raised against the full-length hMis12 produced in bacterial cells. Two independently prepared antisera displayed the same 25-kD band in HeLa cell extracts after affinity purification (Fig. 1 B; unpublished data). To determine whether the 25-kD band really represents hMis12, a plasmid carrying hMis12 under the CMV promoter and tagged with V5His6 (~3 kD) at the COOH terminus was transfected into HeLa cells. The resulting fusion protein band produced in HeLa cells after 24 h was detected by anti-hMis12 and anti-V5 antibodies (Fig. 1 C). Anti-hMis12 antibodies produced two bands (28-kD fusion protein and 25-kD endogenous protein) but anti-V5 antibodies showed only one (28 kD) band. We then constructed plasmids carrying GFP-tagged Mis12 at the COOH (hMis12–GFP) or the NH_2 terminus (GFP–hMis12) and used them for transfection. Protein bands were produced at the expected mol wt (Fig. 1 D) after 12–24 h. No bands, except for the endogenous hMis12, were produced in the control cells (GFP only and nontransfected).

To examine whether the level of hMis12 fluctuates in the cell cycle, HeLa cells arrested at the G1/S or M phase were made and extracts were prepared. Significant changes were not observed between the bands of the exponentially growing state and the arrested G1/S or M phase (Fig. 1 E). The arrested M-phase cells were shown to have increased levels of control mitotic cyclin.

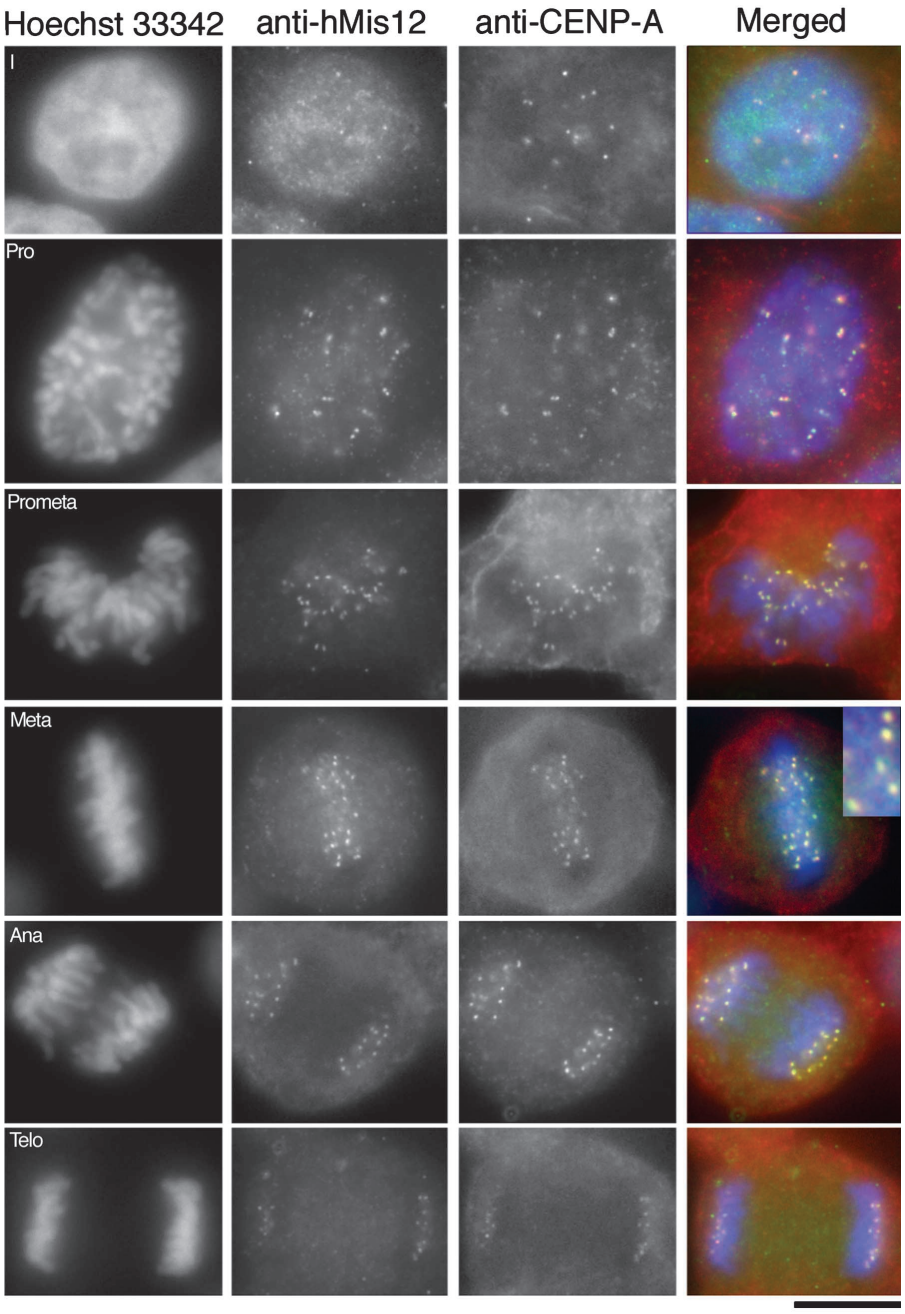

Figure 2. **hMis12 is localized at centromere regions throughout the cell cycle.** Paraformaldehyde-fixed HeLa cells were stained by anti-hMis12 and anti–CENP-A antibodies. DNA was stained by Hoechst 33342. The merged images were produced by hMis12 (green), CENP-A (red), and DNA (blue). hMis12 and CENP-A dots show identical localization patterns throughout the cell cycle, though hMis12 also showed dispersed nuclear signals in interphase. Both hMis12 and CENP-A signals in telophase were rather weak, the reason of which remains unclear. I; interphase, Pro; prophase, Prometa; prometaphase, Meta; metaphase, Ana; anaphase, Telo; telophase. Bar, 10 μm.

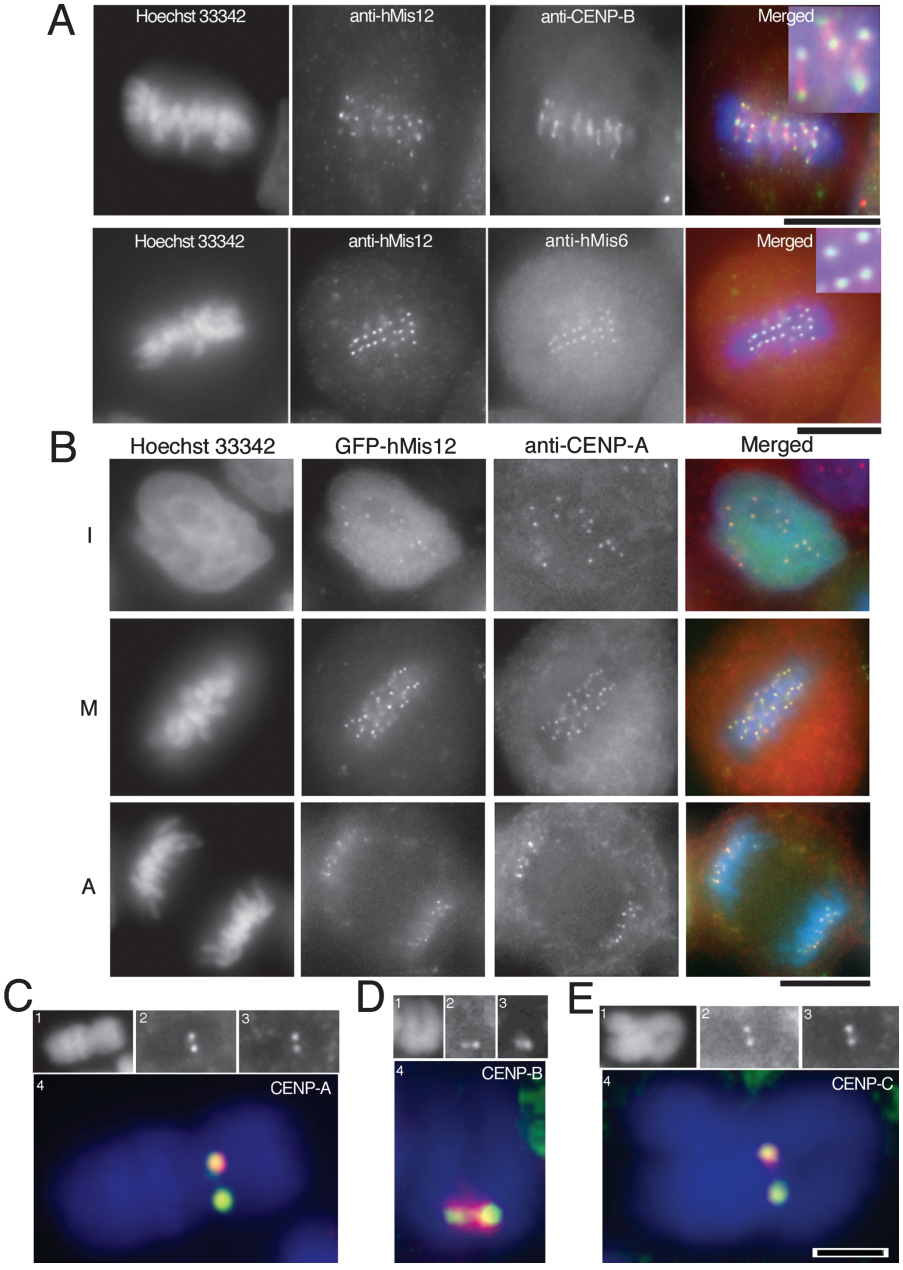

Figure 3. **hMis12 is colocalized with CENP-A and CENP-C.** (A) Coimmunostaining of hMis12 with CENP-B (top), or with hMis6 (bottom) was done. DNA was stained by Hoechst 33342. The merged images were produced by green-colored hMis12, red-colored hMis6 or CENP-B, and blue-colored DNA. hMis12 signals colocalized with hMis6 dots but not CENP-B rod signals in metaphase, as shown in the enlarged images (insets). Bar, 10 μm. (B) GFP–hMis12 is colocalized with CENP-A at centromeres throughout the cell cycle. HeLa cells transfected with GFP–hMis12 were fixed and stained by anti–CENP-A antibody. The merged images were produced by green-colored GFP–hMis12, red-colored CENP-A, and blue-colored DNA. Bar, 10 μm. (C–E) Kinetochore localization of GFP–hMis12 on the spread chromosomes. GFP–hMis12 was expressed in HeLa cells and metaphase spread chromosomes were prepared. Immunostaining of CENP-A (C), CENP-B (D), and CENP-C (E) was performed. hMis12 was colocalized with CENP-A and CENP-C, components of the inner kinetochore plate. Panel 1, chromosome stained by Hoechst 33342; panel 2, GFP-hMis12; panel 3, CENP-A/B/C; panel 4, merged image (blue for chromosome, green for GFP–hMis12, and red for CENPs). Bar, 1 μm.

Localization of hMis12 in the centromere regions

To examine the intracellular localization of hMis12, immunostaining of HeLa cells fixed by paraformaldehyde was performed using affinity-purified anti-hMis12 (Fig. 1 F). For counterstaining, Hoechst 33342 (DNA) and anti-tubulin (TUB) antibodies were also used. Kinetochore-like punctate signals were observed in metaphase and anaphase mitotic cells, which showed condensed chromosomes and the spindle. The punctate signals were not observed in cells stained with preimmune serum. Similar punctate signals were obtained by different fixation (methanol–acetone) or another affinity-purified rabbit antiserum (unpublished data).

To determine whether the signals corresponded to the kinetochores, immunolocalization experiments were done using antibodies against human CENP-A, a variant of histone H3 known to be specifically located at the centromere regions throughout the cell cycle (Palmer et al., 1987; Sullivan et al., 1994; Warburton et al., 1997). As seen in Fig. 2, the punctate signals derived from anti-hMis12 and anti–CENP-A antibodies were identical throughout various mitotic stages. The punctate signals of hMis12 were present on the condensed chromosomes during prophase and prometaphase, congressed at metaphase, and split into two sets during anaphase. This behavior is typical for kinetochore proteins. In interphase, whole chromatin regions were stained by anti-hMis12 antibodies, and, among them, several brighter punctate signals colocalized with CENP-A were visible. Reduction of the cellular hMis12 protein level by the RNAi method described below resulted in the disappearance of both punctate and dispersed nuclear signals, suggesting that both signals were indeed derived from hMis12 protein.

CENP-B was shown to be present in the innermost heterochromatic region of the kinetochores of human chromosomes, whereas CENP-A was located outside of CENP-B at a

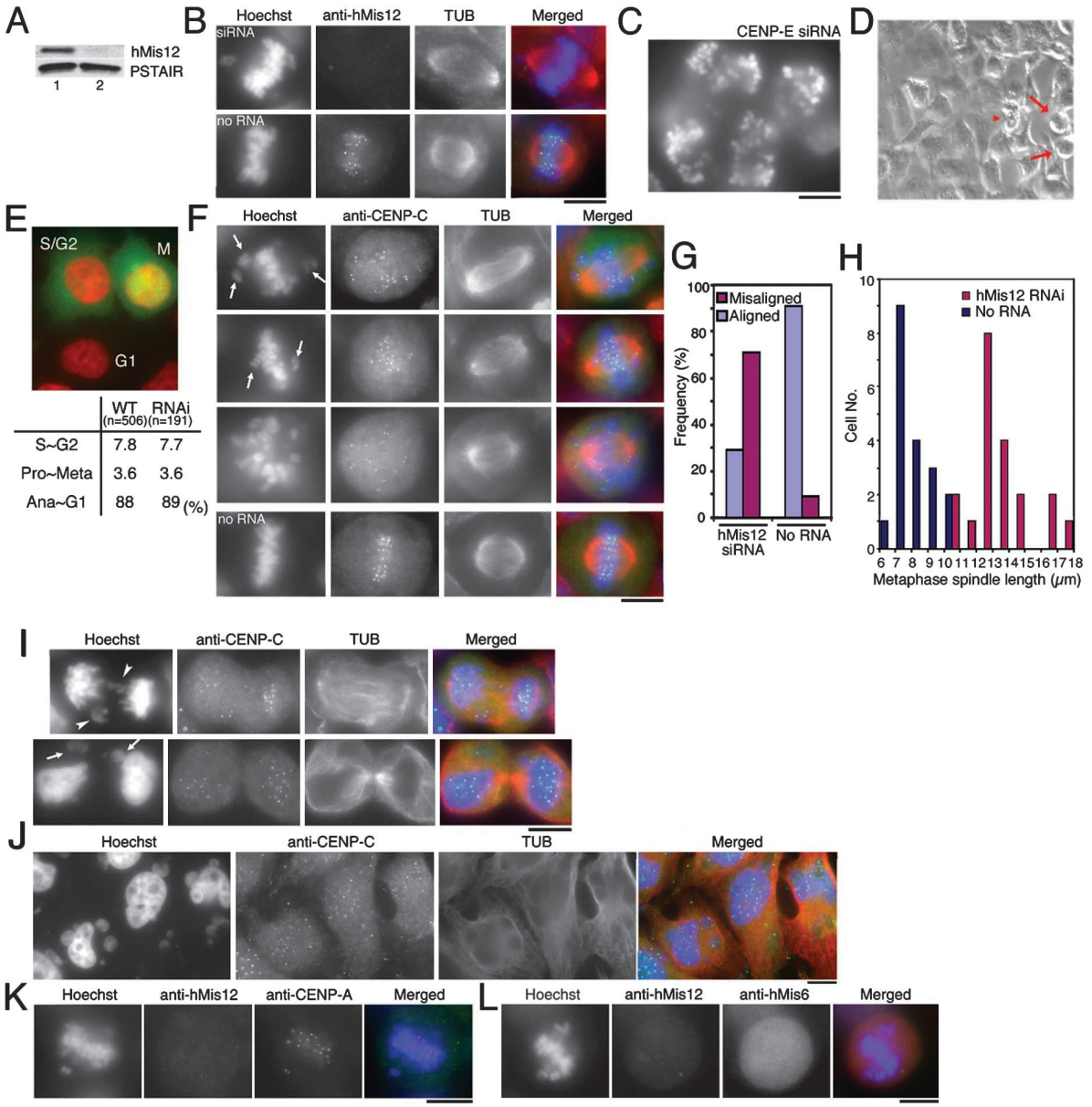

Figure 4. **Metaphase chromosome alignment is impaired by the RNAi method for hMis12.** (A) Immunoblotting of hMis12 in HeLa cell extracts after 85 h. Anti-PSTAIR was used as loading control. The level of hMis12 protein in cell extracts was greatly reduced after incubation with siRNA (lane 2). (B) HeLa cells transfected by siRNA for hMis12 (top) or by control buffer only (bottom) were fixed at 85 h and stained by Hoechst 33342 (blue), anti-hMis12 (green), and anti-tubulin antibodies (red). Centromere signals disappeared by hMis12 RNAi. (C) RNAi for CENP-E induced accumulation of mitotic cells. (D) Micrograph taken by phase contrast. Arrows indicate mitotic cells, whereas cells indicated by arrowheads have an abnormal shape. These abnormally shaped cells were positively detected by the TUNEL assay (not depicted). (E) Immunostaining of cyclin B1 (green). DNA was stained by Hoechst 33342 (red). Frequencies (%) of each population are also shown in the inset table. WT, no RNAi. (F, I, and J) Immunostaining of kinetochores (CENP-C) and tubulin. Cells were fixed 85 h after siRNA transfection. (F) Misaligned chromosomes (arrow) observed in metaphase of hMis12-knockdown cells. (G) Quantitative results indicated that the frequencies of misaligned chromosomes are frequent in metaphase cells after hMis12 RNAi depletion. (H) Quantitative results show that spindles in such hMis12-knockdown cells (red columns) were expanded compared with control nontreated cells. (I, top) Lagging chromosomes (indicated by arrowheads) seen in anaphase cells. (I, bottom) Micronuclei (indicated by arrows) are observed in telophase cells. (J) Micronuclei are frequently seen in interphase cells. (K and L) Kinetochore localization of CENP-A (K) and hMis6 (L) in hMis12-depleted cells. Cells treated with hMis12 siRNA were stained by anti–CENP-A or hMis6 antibodies. Bars, 10 μm.

region called the inner plate (Masumoto et al., 1989; Cooke et al., 1990; Warburton et al., 1997). HeLa cells were fixed by paraformaldehyde and immunostained by anti-hMis12 and anti–CENP-B antibodies. The results shown in Fig. 3 A showed that in metaphase, the signals of hMis12 were rounded dots differing from the rod-like signals of CENP-B, which were located further inside (top row). In the enlarged, merged micrographs, CENP-B (red) was distributed over large areas and clearly distinct from hMis12 (green), which overlapped with the ends of rod-like CENP-B signals.

We next compared the intracellular localization of hMis6 with hMis12. The Mis6 family proteins have been

characterized in both fission and budding yeasts (Saitoh et al., 1997; Measday et al., 2002) and also in chicken (Nishihashi et al., 2002), but not in human. HeLa cells were stained by anti-hMis6 and anti-hMis12 antibodies (Fig. 3 A, bottom). The signals of hMis6 were constitutively in the centromeres in HeLa cells and were colocalized with those of hMis12 in mitosis.

Localization of GFP-tagged hMis12 protein

To confirm that the images obtained by anti-hMis12 antibodies represented centromere proteins, the intracellular localization of hMis12 tagged with GFP was examined. The hMis12 gene was tagged with GFP at the NH_2 terminus (GFP–hMis12) and placed under the CMV promoter, and the resulting plasmid was used for transfection of HeLa cells. The GFP–hMis12 dot signals were identical to those detected by anti–CENP-A antibodies (Fig. 3 B) in interphase (I), metaphase (M), and anaphase (A). No dot-like signals were obtained when only GFP was expressed, it was uniformly present throughout the cell (unpublished data). These results were identical when hMis12 tagged with the COOH terminus was employed (unpublished data). The GFP–hMis12 signals behaved like kinetochores also in time-lapse observation of living mitotic cells (unpublished data).

Precise localization of hMis12 was then determined on spread metaphase-condensed chromosomes. Polyclonal anti-hMis12 antibodies did not show distinct localization on the preparation of the metaphase chromosomes, whereas GFP–hMis12 signals could be clearly observed. Cells transfected with a plasmid carrying GFP–hMis12 were treated with the tubulin poison nocodazole for 18 h followed by osmotic stress to spread condensed chromosomes. Specimens were fixed with paraformaldehyde and immunostained by antibodies against CENP-A (Fig. 3 C), CENP-B (Fig. 3 D), and CENP-C (Saitoh et al., 1992; Warburton et al., 1997; Fig. 3 E). Chromosomes were stained with Hoechst 33342 (Fig. 3, C–E, 1) and observed by GFP–hMis12 (Fig. 3, C–E, 2) and antibodies against CENP-A (Fig. 3 C, 3), CENP-B (Fig. 3 D, 3), and CENP-C (Fig. 3 E, 3). Single punctate signals of GFP–hMis12 (green) were seen on each sister chromatid and positioned identically to CENP-A and CENP-C (merged images, shown in Fig. 3, C–E, 4). The signals of CENP-B were partially overlapped with those of hMis12, but the highly significant intensity was seen inside of the GFP signals on the condensed chromosomes.

Chromosome missegregation in the reduced level of hMis12 by RNAi

To determine the cellular role of hMis12, the RNAi method was employed using the small interfering RNA (siRNA) sequences (see Materials and methods). The amount of hMis12 in HeLa cells was found to be greatly decreased (<20%) after 85 h, whereas the control of no RNA showed the normal level of hMis12 (Fig. 4 A; unpublished data). The control CDK signals (PSTAIR) were not altered in cells treated with siRNA. Fig. 4 B shows immunostained micrographs of HeLa cells after the hMis12 RNAi. Cells transfected with hMis12 siRNA exhibited no signals at the time point (85 h). At earlier time points (48 and 68 h), however, most of the cells still showed centromere and nuclear signals of hMis12 (unpublished data). Detailed observation of hMis12-knockdown cells described below was hence done for the 85-h cells. The siRNA against CENP-E (an outer kinetochore protein) was transfected into HeLa cells as a positive control of the RNAi experiment. Consistent with the previous study (Harborth et al., 2001), mitotic cells with condensed chromosomes were highly accumulated (>80% of total cells; DNA stained in Fig. 4 C).

In sharp contrast, the mitotic index of hMis12-knockdown cells was comparable to nontransfected cells (both were ~8%; Fig. 4 D). Mitotic progression did not appear to be delayed by the hMis12 RNAi. To evaluate cell cycle effects, cyclin B1 staining (Toyoshima et al., 1998) was employed to determine cell cycle stage distributions in hMis12-knockdown cells. Cyclin B1 accumulates in cytoplasm during S and G2, is translocated into the nucleus at prophase, and then disappears by degradation after anaphase through to G1. As shown in Fig. 4 E (with quantitative values in the inset table), the distribution percent frequencies at the three cell cycle stages (S–G2, prophase–metaphase, and anaphase–G1) revealed by cyclin B1 localization after hMis12 RNAi were found to be nearly identical to those in control nontreated cells. The cell cycle progression was thus not blocked by hMis12 reduction.

Aberrant chromosome behavior was, however, frequently observed both in interphase and mitosis of these cells. Fig. 4 (F, I, and J) shows the images of chromosome DNA, kinetochore (CENP-C as a marker), and tubulin in prometa–metaphase (F), anaphase (I), and interphase (J). In mitosis of hMis12-knockdown cells (Fig. 4 F; top three rows), chromosomes were condensed and the metaphase spindle was formed, but typical metaphase images, in which all the chromosomes are aligned at the metaphase plate (Fig. 4 F, bottom row; no RNA transfection), were rarely observed. Instead, DNA masses apart from the metaphase plate were very frequently observed (71% of the metaphase cells, $n = 17$), as shown in Fig. 4 G. These "orphan" DNA masses had CENP-C kinetochore dots, showing that they were misaligned chromosomes. Some CENP-C dots were visible outside the spindle, occasionally near spindle poles. Biorientation of sister kinetochores might be impaired for these sister chromatids. We also found that the metaphase spindle length was 62% longer (13.3 ± 1.8 μm, $n = 20$) in hMis12-knockdown cells than in control cells (8.2 ± 1.0 μm, $n = 19$), as shown in Fig. 4 H.

Contrary to the case of CENP-E RNAi, the abnormality in metaphase cells observed in the cultures treated with the hMis12 siRNA did not result in the mitotic arrest, and cells in the anaphase and telophase stages were clearly observed although they were mostly abnormal. More than 50% of cells containing the anaphase spindle and separating chromosomes had clear lagging chromosomes (Fig. 4 I, arrowheads). Telophase cells displayed micronuclei (Fig. 4 I, arrows). Aberrant micronuclei were abundantly observed in ~60% of interphase cells (examples shown in Fig. 4 J). The formation of these tiny nuclear structures was likely to be the consequence of chromosome missegregation. HeLa cells transfected by buffer only (no RNA) showed negligible levels of micronuclei (<5%). We also found that 4.5% of the total cells ($n = 1,130$) were detached from the culture plate and floated in the medium after

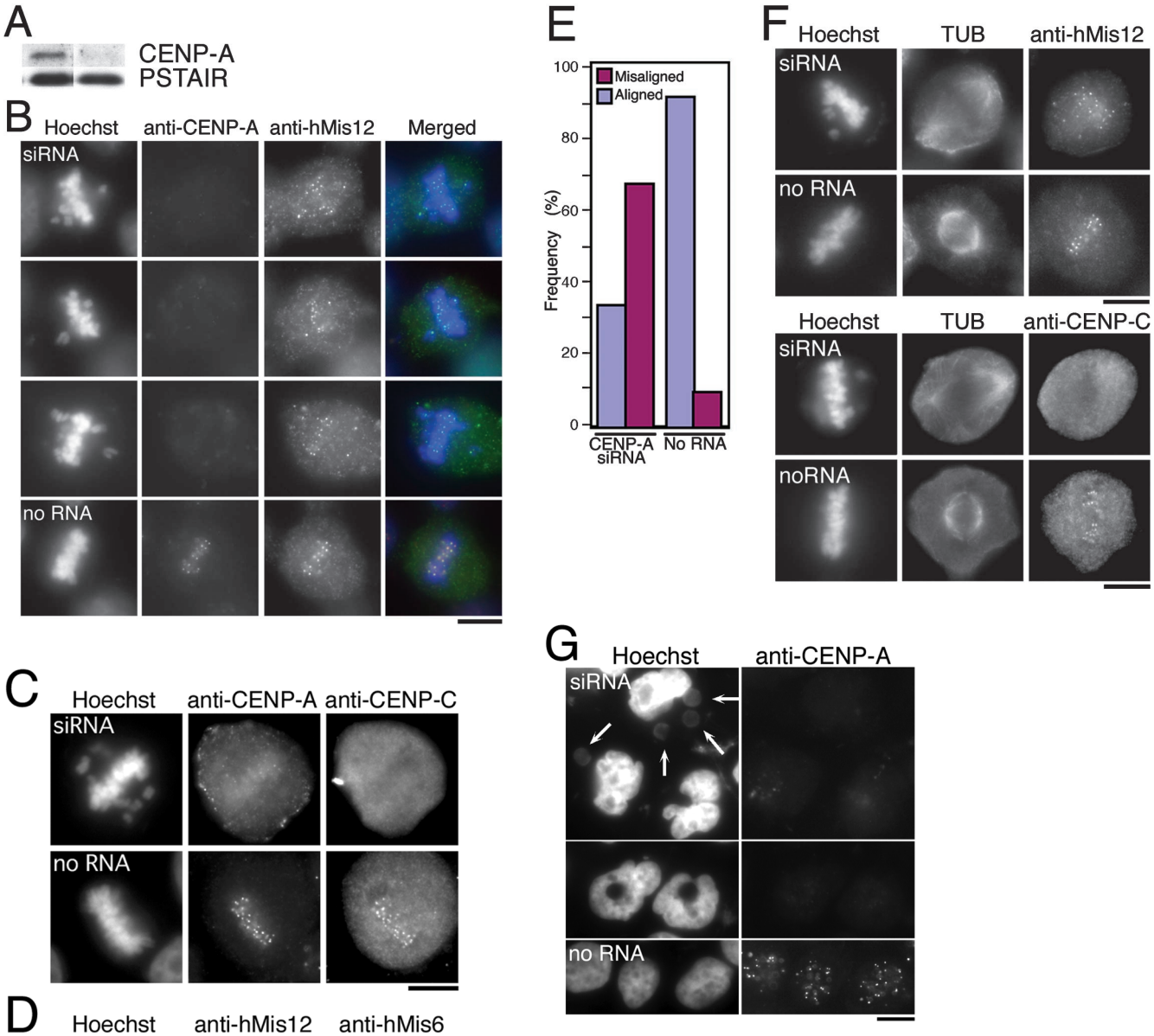

Figure 5. **hMis12 is present at kinetochore after CENP-A depletion by RNAi.** (A) Immunoblotting of CENP-A in HeLa cell extracts after 68 h. Anti-PSTAIR was used as loading control. The level of CENP-A protein in cell extracts was greatly reduced after incubation with siRNA (right), whereas no reduction occurred in control, no RNAi cells (left). (B) HeLa cells transfected by siRNA for CENP-A (top three rows) or by control buffer only (bottom row) were fixed at 68 h and stained by Hoechst 33342 (blue), anti-hMis12 (green), and anti–CENP-A (red) antibodies. Centromere signals of CENP-A, but not of hMis12, disappeared by RNAi. (C) Costaining by anti–CENP-C and anti–CENP-A antibodies. Centromere signals of CENP-C disappeared by CENP-A knockdown. (D) Costaining by anti-hMis6 and anti-hMis12 antibodies. Centromere signals of hMis6 are greatly diminished by CENP-A RNAi. Control, no RNAi cell is shown at bottom. (E) The frequency of misaligned chromosome appearance in CENP-A RNAi and no RNAi, control mitotic cells. Red columns indicate metaphase cells containing aligned chromosomes, and blue columns represent cells not containing aligned chromosomes. (F) Immunostaining by kinetochore marker (hMis12) and tubulin in CENP-A–knockdown mitotic cells. Cells were fixed at 68 h after siRNA transfection. Misaligned chromosomes were frequently observed in CENP-A–knockdown mitotic cells. Mitotic spindles in such cells were greatly expanded compared with control nontreated cells. (G) Micronuclei (arrows) or abnormal donut-shaped nuclei (middle row) seen in CENP-A–reduced interphase cells. Bars, 10 μm.

hMis12 RNAi, which was probably the consequence of cell death (control detached cells, 1.9%). To detect DNA fragmentation during apoptosis, the TUNEL assay was done for cells that remained attached to the plate. The assay showed that apoptosis was induced in only 2.1% of the knockdown cells (n = 1,060) (1.0% in control cells, n = 1049). Round mitotic cells showed no positive signals in the TUNEL assay ($n > 50$), suggesting that the apoptotic event was scarcely induced during mitosis. Aneuploid interphase cells might cause apoptotic cell death. These results indicated that the great reduction of hMis12 led to chromosome missegregation but did not block mitotic progression nor cause mitotic cell death.

CENP-C was kept localized at centromere regions after hMis12 reduction (Fig. 4 F). We then examined the localization of CENP-A and hMis6 under the hMis12 RNAi condition. As shown in Fig. 4 K, CENP-A still exhibited clear dot signals by immunofluorescence in metaphase cells in which hMis12 signals disappeared. CENP-A localization at the centromere seems to not be affected by the reduction of hMis12. In contrast, the centromeric punctate signals of hMis6 were greatly diminished under the hMis12 RNAi condition (Fig. 4 L). Proper localization of hMis6 appears to require hMis12, a situation quite different from that found in fission yeast.

CENP-A acts independently of hMis12 for metaphase chromosome alignment in HeLa cells

The RNAi experiment was done for CENP-A in comparison with the result of hMis12 RNAi. Immunoblot patterns obtained using antibodies against CENP-A showed that the level of cellular CENP-A greatly decreased 68 h after siRNA transfection (Fig. 5 A). Anti–CENP-A immunostaining of HeLa cells treated with the CENP-A siRNA exhibited no signal at this time point (Fig. 5 B). At earlier time points (24 and 48 h), most cells still revealed centromere signals of CENP-A (unpublished data). The detailed observation of CENP-A–knockdown cells described below was hence done for 68-h samples (Fig. 5, B–G).

First, the localization of other kinetochore proteins was investigated in CENP-A–knockdown cells by immunostaining using specific antibodies. In all the cells lacking CENP-A dots ($n > 50$), hMis12 still clearly exhibited punctate signals, although the signal intensity was slightly lower than the control cells (three examples are shown in Fig. 5 B). hMis12 recruitment to kinetochores is thus basically unaffected by the reduction of CENP-A. In sharp contrast, CENP-C showed no punctate signals in CENP-A–knockdown cells but dispersed throughout the cell in mitosis (Fig. 5 C) and interphase (unpublished data). In Fig. 5 D, three examples are shown for the staining of hMis6 in CENP-A RNAi cells (hMis12 was also stained). hMis6 punctate signals were greatly diminished after CENP-A RNAi, whereas intense hMis12 signals remained. Kinetochore localization of hMis6 was thus severely impaired by the depletion of CENP-A, indicating the dependency of hMis6 localization on the presence of CENP-A. The localization of another inner plate component, CENP-H (Sugata et al., 2000), was also examined and found to be no longer punctate but distributed throughout cells (unpublished data), showing that localization of the inner kinetochore proteins, except hMis12, was abolished in the CENP-A RNAi cells.

The mitotic phenotype after CENP-A knockdown was similar to hMis12. Chromosome condensation and spindle formation took place, but misaligned chromosomes were frequently observed in metaphase cells (67%, n = 33), as shown in Fig. 5 E. Anti-tubulin antibody staining (Fig. 5 F) showed that metaphase spindle length was also 55% longer in CENP-A–knockdown cells (12.7 ± 1.9 μm; n = 20) than in control, no RNA cells (8.2 ± 1.0 μm). Accumulation of mitotic cells was not detected however, strongly suggesting that no mitotic delay occurred in the absence of CENP-A. In interphase, the shape of many nuclei (27% of total cells) was deformed or constricted (nuclei in control, no RNA cells were mostly round shaped). Micronuclei similar to those observed in hMis12-knockdown cells (arrows) and also unique donut-shaped nuclei were observed (11.4% and 3.0% of total cells, respectively; Fig. 5 G). These might be the consequence of metaphase misalignment, chromosome missegregation in anaphase, and the defect in the spindle integrity during mitosis. No donut-shaped nuclear staining was observed for hMis12 RNAi, suggesting that the donut-shaped nucleus was specific to CENP-A depletion.

Reduction of hMis6 by RNAi results in mitotic delay

We next analyzed the RNAi phenotype of hMis6 in HeLa cells. This is the first functional analysis of mammalian Mis6, though chicken CENP-I gene disruption analysis was recently reported (Nishihashi et al., 2002). Immunoblot against hMis6 showed that hMis6 protein greatly reduced 48 h after siRNA transfection (Fig. 6 A). Consistently, no kinetochore localization of hMis6 was detected in the transfected cells by immunostaining at this time point (Fig. 6 B). The signal distributed throughout the cell was due to the cross-reaction of anti-hMis6 antibodies, so they did not disappear after RNAi. The localization of other kinetochore proteins was determined by immunostaining after hMis6 RNAi transfection (48 h). As shown in Fig. 6 (B and C), punctate localization of hMis12, CENP-A, and CENP-C was clearly visible after hMis6 depletion, indicating that kinetochore localization of these proteins was unaffected by the reduction of hMis6. Identical results were obtained also in interphase cells. Kinetochore localization of CENP-H, however, was not detected at all in the hMis6 RNAi cells (Fig. 6 D). This CENP-H localization result was a positive control for the RNAi experiment.

The reduction of hMis6 was found to lead to the accumulation of mitotic cells, and at 48 h after siRNA transfection, 35% of the cells (n = 623) were in the mitotic stage, as characterized by round cell shape and condensed chromosomes (Fig. 6, E and F; it was 7.4% in control non-RNA–transfected cells). Anaphase and telophase cells were scarcely observed. Some population of the cells (3%) showed apoptosis-like nuclear structure, which was much less observed in hMis12- or CENP-A–knockdown cells. Fig. 6 G shows three examples of hMis6-depleted cells immunostained using kinetochore marker CENP-C and tubulin. Misaligned chromosome phenotypes, severer than hMis12 or CENP-A RNAi but milder than CENP-E RNAi, were observed in most of the mitotic cells. Condensed chromosomes were scattered both inside and out-

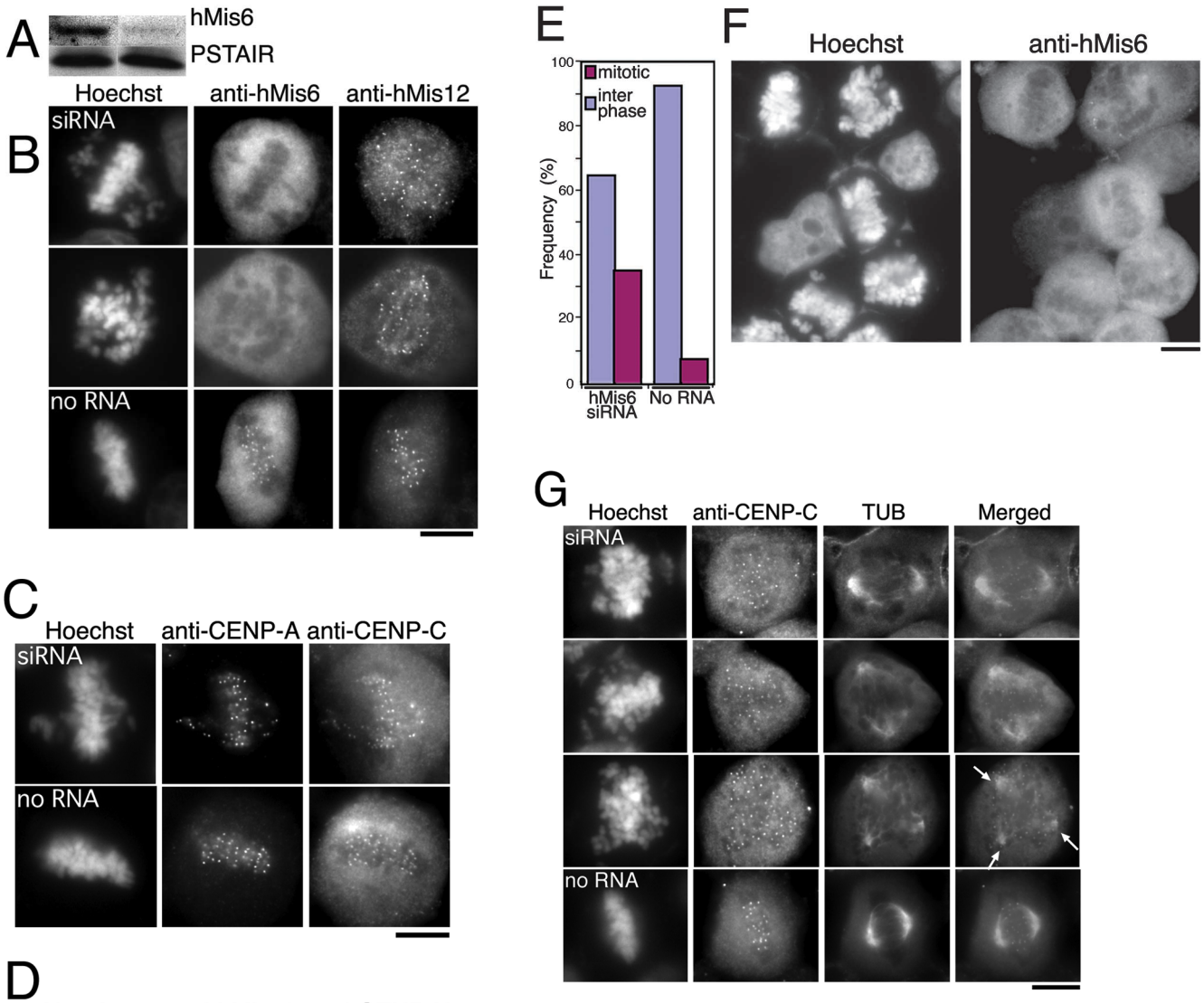

Figure 6. **hMis6 RNAi leads to accumulation of abnormal mitotic cells.** (A) Immunoblotting of hMis6 in HeLa cell extracts after 48 h. Anti-PSTAIR was used as a loading control. The level of hMis6 was greatly reduced after incubation with siRNA (right). No RNAi shown at left. (B) HeLa cells transfected by siRNA for hMis6 (top and middle rows) or by control buffer only (bottom row) were fixed at 48 h and stained by Hoechst 33342, anti-hMis6, and anti-hMis12 antibodies. Centromere signals of hMis6, but not of hMis12, disappeared by RNAi. Misaligned chromosomes were seen by Hoechst staining. (C) Costaining by anti–CENP-A and anti–CENP-C antibodies. Centromere signals of CENP-C remained by hMis6 RNAi. (D) Costaining by anti-hMis12 and anti–CENP-H antibodies. Centromere signals of CENP-H disappeared by hMis6 RNAi. (E) Accumulation of mitotic cells after hMis6 RNAi (red column) in hMis6-depleted cells. Interphase (blue) was abundant in cells not treated by RNAi. (F) Mitotically arrested cells became abundant when HeLa cells were hMis6 depleted. Cells were fixed and stained by Hoechst 33342 and anti-hMis6 antibodies. (G) Immunostaining of kinetochore marker (CENP-C) and tubulin in hMis6-knockdown cells. Cells were fixed 48 h after siRNA transfection. Cells with misaligned chromosomes and expanded bipolar or tripolar spindles (arrows indicate poles) were observed. Bars, 10 μm.

side the spindle. Spindle architecture was also severely impaired, and expanded bipolar spindles (Fig. 6 G, top and middle rows) or tripolar spindles (bottom row; 29.0% of early mitotic cells with spindle) were observed. This mitotic delay phenotype is similar to that observed in the CENP-I gene–disrupted chicken DT40 cell line (Nishihashi et al., 2002).

Temporal kinetochore localization of hMad2 after RNAi against hMis12 or CENP-A

The spindle checkpoint monitors the proper kinetochore–spindle attachment and controls the trigger of metaphase–anaphase transition (for review see Zhou et al., 2002). The localization of hMad2, a conserved spindle checkpoint protein, can be a marker of checkpoint activation, as it is local-

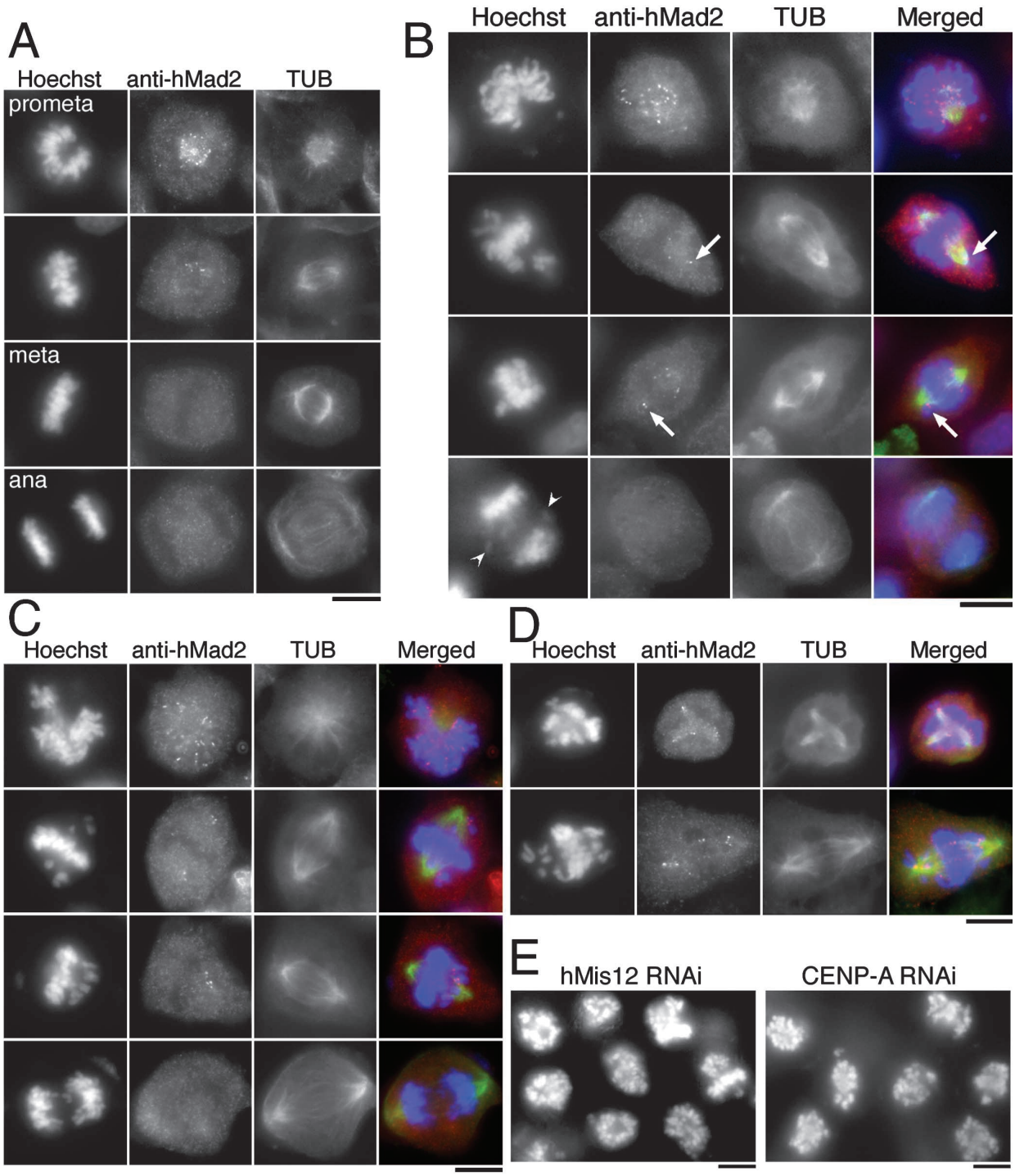

Figure 7. **hMad2 localization after RNAi against hMis12, CENP-A, and hMis6.** (A) hMad2 localization in wild-type HeLa cells. Punctate signals observed in prometaphase disappeared after metaphase. (B and C) hMad2 localization after hMis12 (B) or CENP-A RNAi (C). Dots were observed in most of the misaligned chromosomes (arrows), but invisible on the lagging chromosomes (arrowheads). (D) hMad2 localization after hMis6 RNAi. Dots were visible on the condensed chromosomes in many cases. See text for details. (E) Hoechst 33342 staining of the cells after nocodazole treatment. Nocodazole treatment caused mitotic arrest after hMis12 (85 h) or CENP-A (68 h) RNAi. Bars, 10 μm.

ized at unattached kinetochores and transmits signals that prevent metaphase–anaphase transition (for review see Shah and Cleveland, 2000). In control HeLa cells without siRNA addition, dozens of intense hMad2 punctate signals were observed at kinetochore regions by immunofluorescence during prophase and prometaphase, whereas several or no dots were in metaphase (Fig. 7 A; Chen et al., 1996; Li and Benezra, 1996). No punctate signals were visible on chromosomes after anaphase. We then observed hMad2 localization after RNAi against kinetochore proteins. The localization pattern after the RNAi of hMis12 or CENP-A was similar to control cells: intense kinetochore dots in prophase and prometaphase and several dots on the metaphase-like chromosomes (Fig. 7, B and C). The punctate signals were observed in 73% of the

cells with orphan chromosomes (arrows; $n = 25$), whereas they were not observed after anaphase, even on the lagging chromatids (arrowheads). In the case of hMis6 RNAi, 32% of the mitotic cells had dozens of punctate signals, indicating the prolonged hMad2 localization at kinetochores (Fig. 7 D). It is suggested that the mitotic delay was caused by spindle checkpoint activation. The reason why the remaining 68% of the prometaphase-like hMis6-knockdown cells had no punctate hMad2 signals is unclear.

We next treated cells after RNAi with a high concentration of nocodazole (250 ng/ml) for 12–18 h in order to inhibit spindle formation (the drug was added after 73 h for hMis12 RNAi, 50 h for CENP-A). As shown in Fig. 7 E, most of the cells arrested with condensed chromosomes in response to nocodazole even after the decrease of the protein level. This indicates that the spindle checkpoint could be activated and maintained in hMis12- and CENP-A–deficient cells. This result, together with the temporal kinetochore localization of hMad2, suggests that the spindle checkpoint mechanism per se is at least in part functional after hMis12 or CENP-A RNAi.

Discussion

The present study established that kinetochore protein Mis12, essential for equal segregation of sister chromatids in mitosis, is conserved in eukaryotes. The localization pattern of human hMis12 is indistinguishable (within the resolution of light microscopy) from that of CENP-A, CENP-C, and hMis6, the components of the inner kinetochore plate. Mis12 contains three characteristic sequence features. The NH_2-terminal domain contains two conserved blocks and the coiled coil followed by the nonconserved hydrophilic COOH terminus. These features were kept in all the Mis12 members so far identified (the coiled-coil region was reiterated in *C. albicans*, plant, and animal). The COOH-terminal fragment itself could be located in nuclear chromatin in yeast and human (unpublished data). Our success of Mis12 homologue discovery relied largely upon the careful comparison of overall motif composition, as the E-value obtained was not high. This strategy may be applicable to other kinetochore proteins whose homologues have been found only in fungi.

In the present study, functional analysis of hMis12 was done together with hMis6 and CENP-A by the RNAi method using HeLa cells (Elbashir et al., 2001), as comparative study was thought to be essential for proper interpretation. The phenotypes by RNAi are similar between hMis12 and CENP-A. The reduction in the level of hMis12 and CENP-A by transfection of siRNA induced the high frequency of misaligned metaphase chromosomes and lagging chromosomes in anaphase, followed by the frequent appearance of micronuclei in interphase. These mitotic and interphase abnormalities probably reflect chromosome missegregation and aneuploidy, which are frequently observed in tumor cells (Sen, 2000). Our CENP-A RNAi result is not inconsistent with the phenotypes reported for CENP-A knockout mice (Howman et al., 2000). The phenotypic variability, some cells display partial metaphase alignment and others show almost no alignment (Fig. 4 F), might reflect variability in the levels of residual hMis12 in individual cells after siRNA transfection.

The metaphase spindle size is strikingly expanded in hMis12- and CENP-A–depleted cells. As the spindle expansion phenotype is found for fission yeast mutants *mis12* and *mis6* and also in budding yeast *mtw1* (Goshima et al., 1999; Goshima and Yanagida, 2000), the metaphase spindle size is under the control of kinetochore chromatin proteins in both human and yeast. It is an important conclusion that the small kinetochore chromatin determines the large size of the human metaphase spindle. It was previously shown that microtubules form the spindle by sensing the concentration gradient of a chromatin protein, RCC1, the GTP exchange factor for Ran (Carazo-Salas et al., 1999; Kalab et al., 2002). The spindle length seems to be directed by chromosomal proteins that are situated at the kinetochores. The longer than normal metaphase spindle may induce abnormal behavior of kinetochores during prometa and metaphase, leading to missegregation. Consistently, fission yeast extragenic suppressor mutants could reduce the length of the mutant metaphase spindle (unpublished data).

It was surprising that the spindle checkpoint delay was apparently not observed in the hMis12- and CENP-A–reduced HeLa cells. Meanwhile, those cells could stop mitotic progression upon their spindle disruption. A simple hypothesis to reconcile these results is that the checkpoint mechanism per se is intact and the attachment of kinetochore microtubules to kinetochores occurred in hMis12- and CENP-A–reduced HeLa cells so that the checkpoint delay does not occur. Some kinds of kinetochore protein defects may be "overlooked" by the checkpoint mechanism, followed by missegregation with lagging chromosomes at anaphase. Temporal kinetochore localization of hMad2 after RNAi, similar to the case of wild type, is not inconsistent with this model. It was recently shown that merotelic attachment of kinetochore microtubules is the possible cause for lagging chromosome and subsequent aneuploidy in vertebrates and that this abnormal attachment was not detected by checkpoint mechanisms (Cimini et al., 2001, 2002). It would be possible that the misaligned chromosomes shown here have merotelic attachment due to the kinetochore chromatin disruption. The distinct type of misaligned chromosomes that often activate the spindle checkpoint and produce "wait anaphase" signals in vertebrate cells (Rieder and Salmon, 1998) may be applied to monooriented chromosomes.

Another possibility is that the disruption of kinetochore chromatin by the RNAi of hMis12 and CENP-A may lead to a deficiency in kinetochore–spindle attachment and also in the activation and maintenance of the kinetochore-based checkpoint. If, however, the whole spindle structure is disrupted by a tubulin poison, the spindle checkpoint could still be activated. The RNAi phenotypes might be explained by the kinetochore-specific checkpoint model that hMis12 and CENP-A are essential for prolonged kinetochore localization of hMad2, for example.

A principal conclusion in the present study is that kinetochore localization dependency does not appear to exist between CENP-A and hMis12 in HeLa cells. The same independent behavior was found in fission yeast (Takahashi et al., 2000). Fission yeast and human Mis12 are localized in the kinetochores in CENP-A–knockdown cells. Fig. 8 summarizes the localization dependency of kinetochore proteins in HeLa

A

RNAi	hMis12	CENP-A	hMis6	CENP-C	CENP-H
hMis12	-	+	-	+	-
CENP-A	+	-	-	-	-
hMis6	+	+	-	+	-

+: Persistent kinetochore localisation
- : Loss of kinetochore localisation

B

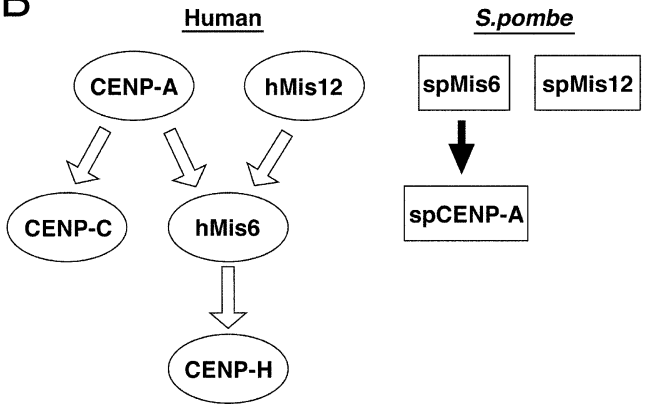

Figure 8. **Localization dependencies of kinetochore proteins hMis12, CENP-A, hMis6, CENP-C, and CENP-H in HeLa cells revealed by the RNAi method.** (A) Results of intracellular localization of five kinetochore proteins in three different RNAi knockdowns are summarized. The localization of hMis12 and CENP-A is independent. (B) Localization dependency of kinetochore proteins in human and *S. pombe* is illustrated. The arrows indicate the requirement of functional kinetochore protein for proper localization of the downward proteins. In *S. pombe*, the localization of spMis12 and spCENP-A is independent, but the directionality for the requirements of Mis6 and CENP-A is different (Takahashi et al., 2000). The reason for this difference is unclear.

cells revealed by this study. CENP-A localization does not require hMis6. Instead, the localization of hMis6 at the centromere needs both hMis12 and CENP-A. This is very different from the case of fission yeast in which spMis6 is essential for spCENP-A loading, and neither spCENP-A nor spMis12 is required for kinetochore localization of Mis6 (Goshima et al., 1999; Takahashi et al., 2000). The reason for this striking difference is unclear. In regard to CENP-C, its kinetochore localization depends on CENP-A, but not on hMis6, differing from the properties reported for chicken (Nishihashi et al., 2002). Dependency of localization for the case of CENP-C is not conserved, even among vertebrates. hMis12 is thus the first example that shows identical localization to CENP-A, but independently of the presence of functional CENP-A in multicellular organisms (Howman et al., 2000; Blower and Karpen, 2001; Oegema et al., 2001). This may suggest that CENP-A is not the sole inner chromatin core and that CENP-A RNAi does not necessarily result in the "kinetochore-null" phenotype in humans, as hMis12 is still capable of being recruited to the kinetochore. Mis12 seems to form a loading pathway distinct from that of CENP-A. One may argue that a residual amount of CENP-A that could not be detected by immunofluorescence might be sufficient to allow localization of hMis12. This is always the potential problem in any kind of functional analyses of essential genes, even in the yeast gene disruption experiment, because 100% depletion of an essential protein from a cell is impossible (the yeast gene-disrupted spores often contain protein derived from zygotes). It is hence not completely ruled out that the residual CENP-A (10% or less) not detected by immunostaining may be sufficient to allow nearly full localization of hMis12. In the present study, the clear disappearance of CENP-C, CENP-H, and hMis6 from kinetochores after CENP-A RNAi strongly supports the model that hMis12 is classified into a functionally different group from the CENP-A pathway in the kinetochore assembly process.

What kind of independent pathway may be considered for the Mis12 protein family? The work on *S. pombe* shows that spMis12, a phosphoprotein, is regulated by a protein phosphatase and that spMis12 may be implicated in ubiquitination and proteolysis by forming an oligomeric complex with two or three other kinetochore chromatin proteins (unpublished data). The answer to the question of whether human hMis12 shows similar behavior awaits future investigation.

Materials and methods

Strains and media

HeLa cells were grown at 37°C in DME (GIBCO BRL) supplemented with 10% FCS, 1% penicillin–streptomycin, and 1% antibiotic–antimycotic.

Plasmids and transfection

The human hMis12 gene was cloned by direct PCR using a HeLa cDNA library as template. GFP–hMis12 plasmid was constructed by inserting the whole coding region of hMis12 in frame into pEGFP-C1 vector (CMV promoter; CLONTECH Laboratories, Inc.) by introducing a BglII site in front of the initiation codon and a NotI site after the stop codon. The ampicillin resistance gene was then added for selection. Plasmid hMis12-V5His6 was made by inserting the hMis12 sequence (having BglII and SacII sites introduced before the initiation and after the termination codon, respectively) in frame into plasmid pcDNA3.1/V5His6 (CMV promoter; Invitrogen). Plasmid DNAs were purified using the Endofree Maxi kit (QIAGEN) and transfected into HeLa cells by the Effectene transfection kit (QIAGEN).

Antibodies

To obtain polyclonal antibodies against human Mis12 protein, the full-length 205-aa sequence of the hMis12 gene was inserted in frame into pGST vector. GST–hMis12 was produced in *Escherichia coli* with induction of expression by 1 mM IPTG for 4 h at 36°C. The fusion protein recovered in the inclusion bodies was sonicated, separated by SDS-PAGE, and electro-eluted by BIOTRAP (Schleicher & Schuell). This step was repeated twice. The purified GST–hMis12 protein was used for the immunization of two rabbits, and polyclonal antisera were obtained. The 13-wk sera were affinity purified using membranes on which recombinant GST–hMis12 was blotted.

Immunofluorescence

HeLa cells were fixed with PFA solution (PBS containing 3% paraformaldehyde and 2% sucrose) for 10 min at room temperature and then permeabilized with 0.5% Triton X-100 for 5 min on ice. After washing three times with PBS, fixed cells were pretreated with PBS containing 1% BSA (or 0.1% BSA/0.1% skim milk) for 10 min, followed by incubation with primary antibodies (anti-hMis12[rabbit, 1:30], anti–CENP-A [A3, mouse, 1:100], anti-tubulin [DM1A, mouse, 1:500], anti–CENP-C [guinea pig, 1:1,000], anti–CENP-B [mouse, 1:2], anti-hMis6 [1:500]), anti-Mad2 [rabbit, 1:500; COVANCE], anti-cyclin B1 [GNS1, 1:100; Santa Cruz Biotechnology, Inc.]) and secondary antibodies (labeled with Alexa®468, Alexa®546, or rhodamine). For staining cellular DNA, 0.5 μg/ml Hoechst 33342 was used. The TUNEL assay was performed using an in situ apoptosis detection kit (Takara).

Mitotic chromosome spread

The procedure described in Hoque and Ishikawa (2001) was followed with slight modifications. HeLa cells transfected with pGFP-hMis12 were cul-

tured for 18 h in the presence of 250 ng/ml nocodazole (Sigma-Aldrich). Accumulated mitotic cells were then harvested, treated with a hypotonic buffer (10 mM Tris-Cl, pH 7.5, 10 mM NaCl, 5 mM $MgCl_2$) for 10 min at 37°C, and attached to micro coverglass. The cells on the glass were fixed with PFA solution as described above, followed by immunofluorescence.

RNAi method

siRNA (Elbashir et al., 2001) was synthesized for RNAi of hMis12 (5′-GGACAUUUUGAUAACCUUUTT-3′), CENP-A (5′-CACAGUCGGCGGAGACAAGTT-3′), and hMis6 (5′-GCAACUCGAAGAACAUCUCTT-3′) by JbioS. The sequences are unique in the human genome database. For positive control, the RNA sequence for CENP-E (Harborth et al., 2001) was used. The procedures of cell culture and transfection were based on Elbashir et al. (2001) and Harborth et al. (2001) using Oligofectamine (Invitrogen). HeLa cells (5–20% confluency) were transfected at 0 h. Cells for immunoblotting and fluorescence microscopy were collected after 48–85 h. The levels of hMis12, CENP-A, and hMis6 dramatically decreased after 85, 68, and 48 h, respectively. For RNAi of CENP-E, mitotic cells were found to be accumulated 24 h after transfection as reported previously (Harborth et al., 2001).

We are greatly indebted to Steven Henikoff and Jorja Henikoff for the method of database search, Hiroshi Masumoto (Nagoya University) for anti–CENP-B antibodies, Kazuo Todokoro (RIKEN, Tsukuba, Japan) for anti–CENP-H antibodies, and Kohta Takahashi (Kurume University, Kurume, Japan), Tomohiro Matsumoto, Toshiyuki Habu, Fumiko Toyoshima-Morimoto, Yutaka Matsubayashi, and Shin Yonehara (Kyoto University) for mammalian cell manipulation.

This work is supported by the COE Scientific Research Grant from the Ministry of Education, Culture, Sports, Science, and Technology. G. Goshima was the recipient of a pre- and post-doctoral fellowship of Japan Science Promotion Science.

Submitted: 1 October 2002
Revised: 18 November 2002
Accepted: 21 November 2002

References

Bailey, T.L., and M. Gribskov. 1998. Methods and statistics for combining motif match scores. *J. Comput. Biol.* 5:211–221.

Bernard, P., J.F. Maure, J.F. Partridge, S. Genier, J.P. Javerzat, and R.C. Allshire. 2001. Requirement of heterochromatin for cohesion at centromeres. *Science.* 294:2539–2542.

Blower, M.D., and G.H. Karpen. 2001. The role of *Drosophila* CID in kinetochore formation, cell-cycle progression and heterochromatin interactions. *Nat. Cell Biol.* 3:730–739.

Carazo-Salas, R.E., G. Guarguaglini, O.J. Gruss, A. Segref, E. Karsenti, and I.W. Mattaj. 1999. Generation of GTP-bound Ran by RCC1 is required for chromatin-induced mitotic spindle formation. *Nature.* 400:178–181.

Cheeseman, I.M., D.G. Drubin, and G. Barnes. 2002. Simple centromere, complex kinetochore: linking spindle microtubules and centromeric DNA in budding yeast. *J. Cell Biol.* 157:199–203.

Chen, R.H., J.C. Waters, E.D. Salmon, and A.W. Murray. 1996. Association of spindle assembly checkpoint component XMAD2 with unattached kinetochores. *Science.* 274:242–246.

Choo, K.H. 2001. Domain organization at the centromere and neocentromere. *Dev. Cell.* 1:165–177.

Cimini, D., B. Howell, P. Maddox, A. Khodjakov, F. Degrassi, and E.D. Salmon. 2001. Merotelic kinetochore orientation is a major mechanism of aneuploidy in mitotic mammalian tissue cells. *J. Cell Biol.* 153:517–527.

Cimini, D., D. Fioravanti, E.D. Salmon, and F. Degrassi. 2002. Merotelic kinetochore orientation versus chromosome mono-orientation in the origin of lagging chromosomes in human primary cells. *J. Cell Sci.* 115:507–515.

Cooke, C.A., R.L. Bernat, and W.C. Earnshaw. 1990. CENP-B: a major human centromere protein located beneath the kinetochore. *J. Cell Biol.* 110:1475–1488.

Ekwall, K., J.P. Javerzat, A. Lorentz, H. Schmidt, G. Cranston, and R. Allshire. 1995. The chromodomain protein Swi6: a key component at fission yeast centromeres. *Science.* 269:1429–1431.

Elbashir, S.M., J. Harborth, W. Lendeckel, A. Yalcin, K. Weber, and T. Tuschl. 2001. Duplexes of 21-nucleotide RNAs mediate RNA interference in cultured mammalian cells. *Nature.* 411:494–498.

Fire, A., S. Xu, M.K. Montgomery, S.A. Kostas, S.E. Driver, and C.C. Mello. 1998. Potent and specific genetic interference by double-stranded RNA in *Caenorhabditis elegans*. *Nature.* 391:806–811.

Fitzgerald-Hayes, M., L. Clarke, and J. Carbon. 1982. Nucleotide sequence comparisons and functional analysis of yeast centromere DNAs. *Cell.* 29:235–244.

Goshima, G., and M. Yanagida. 2000. Establishing biorientation occurs with precocious separation of the sister kinetochores, but not the arms, in the early spindle of budding yeast. *Cell.* 100:619–633.

Goshima, G., S. Saitoh, and M. Yanagida. 1999. Proper metaphase spindle length is determined by centromere proteins Mis12 and Mis6 required for faithful chromosome segregation. *Genes Dev.* 13:1664–1677.

Harborth, J., S.M. Elbashir, K. Bechert, T. Tuschl, and K. Weber. 2001. Identification of essential genes in cultured mammalian cells using small interfering RNAs. *J. Cell Sci.* 114:4557–4565.

Henikoff, S., S. Pietrokovski, and J.G. Henikoff. 1998. Superior performance in protein homology detection with the Blocks Database servers. *Nucleic Acids Res.* 26:309–312.

Hoque, M.T., and F. Ishikawa. 2001. Human chromatid cohesin component hRad21 is phosphorylated in M phase and associated with metaphase centromeres. *J. Biol. Chem.* 276:5059–5067.

Howman, E.V., K.J. Fowler, A.J. Newson, S. Redward, A.C. MacDonald, P. Kalitsis, and K.H. Choo. 2000. Early disruption of centromeric chromatin organization in centromere protein A (Cenpa) null mice. *Proc. Natl. Acad. Sci. USA.* 97:1148–1153.

Kalab, P., K. Weis, and R. Heald. 2002. Visualization of a Ran-GTP gradient in interphase and mitotic *Xenopus* egg extracts. *Science.* 295:2452–2456.

Kitagawa, K., and P. Hieter. 2001. Evolutionary conservation between budding yeast and human kinetochores. *Nat. Rev. Mol. Cell Biol.* 2:678–687.

Li, Y., and R. Benezra. 1996. Identification of a human mitotic checkpoint gene: hsMAD2. *Science.* 274:246–248.

Maeda, I., Y. Kohara, M. Yamamoto, and A. Sugimoto. 2001. Large-scale analysis of gene function in *Caenorhabditis elegans* by high-throughput RNAi. *Curr. Biol.* 11:171–176.

Masumoto, H., H. Masukata, Y. Muro, N. Nozaki, and T. Okazaki. 1989. A human centromere antigen (CENP-B) interacts with a short specific sequence in alphoid DNA, a human centromeric satellite. *J. Cell Biol.* 109:1963–1973.

Measday, V., D.W. Hailey, I. Pot, S.A. Givan, K.M. Hyland, G. Cagney, S. Fields, T.N. Davis, and P. Hieter. 2002. Ctf3p, the Mis6 budding yeast homolog, interacts with Mcm22p and Mcm16p at the yeast outer kinetochore. *Genes Dev.* 16:101–113.

Nishihashi, A., T. Haraguchi, Y. Hiraoka, T. Ikemura, V. Regnier, H. Dodson, W.C. Earnshaw, and T. Fukagawa. 2002. CENP-I is essential for centromere function in vertebrate cells. *Dev. Cell.* 2:463–476.

Nonaka, N., T. Kitajima, S. Yokobayashi, G. Xiao, M. Yamamoto, S.I. Grewal, and Y. Watanabe. 2002. Recruitment of cohesin to heterochromatic regions by Swi6/HP1 in fission yeast. *Nat. Cell Biol.* 4:89–93.

Oegema, K., A. Desai, S. Rybina, M. Kirkham, and A.A. Hyman. 2001. Functional analysis of kinetochore assembly in *Caenorhabditis elegans*. *J. Cell Biol.* 153:1209–1226.

Palmer, D.K., K. O'Day, M.H. Wener, B.S. Andrews, and R.L. Margolis. 1987. A 17-kD centromere protein (CENP-A) copurifies with nucleosome core particles and with histones. *J. Cell Biol.* 104:805–815.

Partridge, J.F., B. Borgstrom, and R.C. Allshire. 2000. Distinct protein interaction domains and protein spreading in a complex centromere. *Genes Dev.* 14:783–791.

Polizzi, C., and L. Clarke. 1991. The chromatin structure of centromeres from fission yeast: differentiation of the central core that correlates with function. *J. Cell Biol.* 112:191–201.

Rieder, C.L., and E.D. Salmon. 1998. The vertebrate cell kinetochore and its roles during mitosis. *Trends Cell Biol.* 8:310–318.

Saitoh, H., J. Tomkiel, C.A. Cooke, H. Ratrie III, M. Maurer, N.F. Rothfield, and W.C. Earnshaw. 1992. CENP-C, an autoantigen in scleroderma, is a component of the human inner kinetochore plate. *Cell.* 70:115–125.

Saitoh, S., K. Takahashi, and M. Yanagida. 1997. Mis6, a fission yeast inner centromere protein, acts during G1/S and forms specialized chromatin required for equal segregation. *Cell.* 90:131–143.

Schueler, M.G., A.W. Higgins, M.K. Rudd, K. Gustashaw, and H.F. Willard. 2001. Genomic and genetic definition of a functional human centromere. *Science.* 294:109–115.

Sen, S. 2000. Aneuploidy and cancer. *Curr. Opin. Oncol.* 12:82–88.

Shah, J.V., and D.W. Cleveland. 2000. Waiting for anaphase: Mad2 and the spindle assembly checkpoint. *Cell.* 103:997–1000.

Sugata, N., S. Li, W.C. Earnshaw, T.J. Yen, K. Yoda, H. Masumoto, E. Munekata, P.E. Warburton, and K. Todokoro. 2000. Human CENP-H multimers colocalize with CENP-A and CENP-C at active centromere–kinetochore complexes. *Hum. Mol. Genet.* 9:2919–2926.

Sullivan, K.F., M. Hechenberger, and K. Masri. 1994. Human CENP-A contains a histone H3 related histone fold domain that is required for targeting to the centromere. *J. Cell Biol.* 127:581–592.

Sun, X., J. Wahlstrom, and G. Karpen. 1997. Molecular structure of a functional *Drosophila* centromere. *Cell.* 91:1007–1019.

Takahashi, K., S. Murakami, Y. Chikashige, H. Funabiki, O. Niwa, and M. Yanagida. 1992. A low copy number central sequence with strict symmetry and unusual chromatin structure in fission yeast centromere. *Mol. Biol. Cell.* 3:819–835.

Takahashi, K., E.S. Chen, and M. Yanagida. 2000. Requirement of Mis6 centromere connector for localizing a CENP-A-like protein in fission yeast. *Science.* 288:2215–2219.

Toyoshima, F., T. Moriguchi, A. Wada, M. Fukuda, and E. Nishida. 1998. Nuclear export of cyclin B1 and its possible role in the DNA damage-induced G2 checkpoint. *EMBO J.* 17:2728–2735.

Warburton, P.E., C.A. Cooke, S. Bourassa, O. Vafa, B.A. Sullivan, G. Stetten, G. Gimelli, D. Warburton, C. Tyler-Smith, K.F. Sullivan, et al. 1997. Immunolocalization of CENP-A suggests a distinct nucleosome structure at the inner kinetochore plate of active centromeres. *Curr. Biol.* 7:901–904.

Zhou, J., J. Yao, and H.C. Joshi. 2002. Attachment and tension in the spindle assembly checkpoint. *J. Cell Sci.* 115:3547–3555.